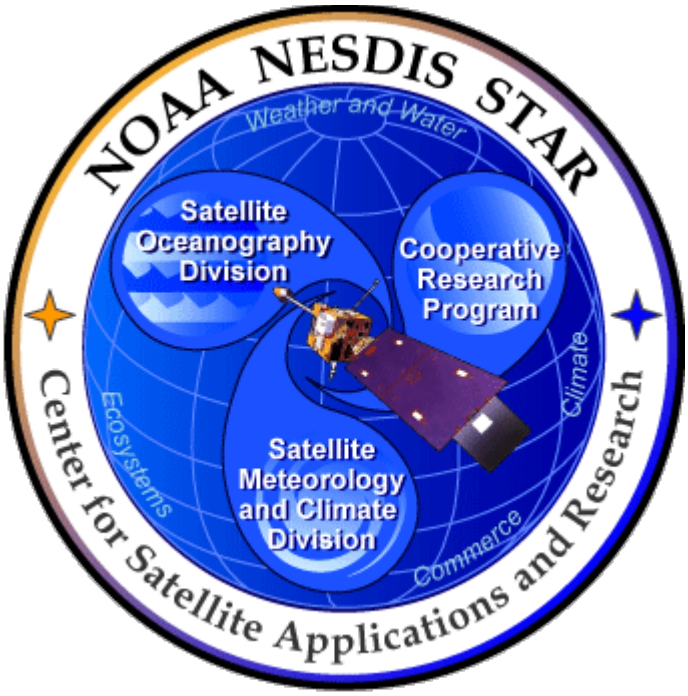

NOAA NESDIS
CENTER for SATELLITE APPLICATIONS and RESEARCH

ALGORITHM THEORETICAL BASIS DOCUMENT

Ice Motion from ABI, VIIRS, AMSR2, and METimage

Aaron Letterly, UW/CIMSS
Yinghui Liu, UW/CIMSS
Jeff Key, NOAA/NESDIS/STAR

Version 2.3
September 13, 2020

TABLE OF CONTENTS

LIST OF FIGURES

LIST OF TABLES

LIST OF ACRONYMS

ABI: Advanced Baseline Imager
AIM: ABI Ice Motion
AIT: Algorithm Integration Team
AMSR2: Advanced Microwave Scanning Radiometer 2
ATBD: Algorithm Theoretical Basis Document
AWG: Algorithm Working Group
BT: Brightness Temperature
CIMSS: Cooperative Institute for Meteorological Satellite Studies
EASE: Equal-Area Scalable Earth
EPS-SG: EUMETSAT Polar System- Second Generation
EUMETSAT: European Organisation for the Exploitation of Meteorological Satellites
FFT: Fast Fourier transforms
GOES-R: Geostationary Operational Environmental Satellite R series MODIS: Moderate Resolution Imaging Spectroradiometer
IABP: International Arctic Buoy Program
JPSS: Joint Polar Satellite System
MODIS: Moderate Resolution Imaging Spectroradiometer
MRD: Mission Requirements Document
MS2GT: MODIS Swath-to-Grid Toolbox
MCC: Maximum Cross-Correlation
MRD: Mission Requirements Document
NH: Northern Hemisphere
NIC: National Ice Center
NOAA: National Oceanic and Atmospheric Administration
SAR: synthetic-aperture-radar
S-NPP: Suomi National Polar Orbiting Partnership
VII: Visible Infrared Imager
VIIRS: Visible Infrared Imaging Radiometer Suite

ABSTRACT

The cryosphere exists at all latitudes and in about one hundred countries. It has profound socio-economic value due to its role in water resources and its impact on transportation, fisheries, hunting, herding, and agriculture. It also plays a significant role in climate studies and is critical for accurate weather forecasts. Ice motion is an important property of ice cover in the cryosphere. This document provides a high-level description of the physical basis and technical approach of an algorithm to retrieve ice motion vectors under clear conditions from the Advanced Baseline Imager (ABI) on the Geostationary Operational Environmental Satellite R series (GOES-R) of National Oceanic and Atmospheric Administration (NOAA) geostationary meteorological satellites. A maximum cross-correlation procedure is applied to two images covering the same area but separated in time in order to retrieve the ice motion vectors. This algorithm can be applied to multiple sensors on multiple satellite platforms, e.g. the Advanced Baseline Imager (ABI) on the Geostationary Operational Environmental Satellite R series (GOES-R) of National Oceanic and Atmospheric Administration (NOAA) geostationary meteorological satellites, the Visible Infrared Imaging Radiometer Suite (VIIRS) onboard the Suomi National Polar Orbiting Partnership (S-NPP) and the Joint Polar Satellite System (JPSS), and METimage (also called Visible Infrared Imager or VII) to be integrated in the EUMETSAT Polar System-Second Generation (EPS-SG) or Metop-SG. Validation studies show that the results meet the requirements of product measurement accuracy and precision. It is expected that this will become NOAA's "Enterprise" algorithm for ice motion.

1 INTRODUCTION

1.1 Purpose of This Document

This ice motion algorithm theoretical basis document (ATBD) provides a high-level description of the physical basis for detection of movement of the ice, and estimation of the speed and direction of ice motion with data from various satellite imagers, e.g. the Advanced Baseline Imager (ABI) on the Geostationary Operational Environmental Satellite R series (GOES-R) of National Oceanic and Atmospheric Administration (NOAA) geostationary meteorological satellites, the Visible Infrared Imaging Radiometer Suite (VIIRS) onboard the Suomi National Polar Orbiting Partnership (S-NPP) and the Joint Polar Satellite System (JPSS), and METimage (also called Visible Infrared Imager or VII) to be integrated in the EUMETSAT Polar System-Second Generation (EPS-SG) or Metop-SG. It is expected that this will become NOAA's "Enterprise" algorithm for ice motion.

1.2 Who Should Use This Document

The intended users of this document are those interested in understanding the physical basis and technical implementation of the algorithms, and how to use the output of this algorithm for a particular application. This document also provides information useful to anyone implementing, maintaining, and potentially improving the original algorithm.

1.3 Inside Each Section

This document is broken down into the following main sections.

- **System Overview**: Provides relevant details of the ABI and provides a brief description of the products generated by the algorithm.

- **Algorithm Description**: Provides a detailed description of the algorithm including its physical basis, input, and output.

- **Assumptions and Limitations**: Provides an overview of the current limitations of the approach and presents the plan for overcoming these limitations with further algorithm development.

1.4 Related Documents

This document currently does not relate to any other document besides the GOES-R Mission Requirements Document (MRD) and the references given throughout.

1.5 Revision History

Version 0.2 of this document was created by William Straka III and Yinghui Liu, Cooperative Institute for Meteorological Satellite Studies (CIMSS), University of Wisconsin-Madison, and Jeffrey Key of NOAA/NESDIS. It is intended to accompany the delivery of the version 0.0 algorithm to the GOES-R Algorithm Working Group (AWG) Algorithm Integration Team (AIT). Version 1.0 was updated by Yinghui Liu and Jeffrey

Key for the 80% ATBD submitted to AIT. Version 2.0 was modified by Yinghui Liu and Jeffrey Key for the 100% ATBD draft submitted to AIT. Version 2.1 is the final 100% ATBD. Version 2.2 was created by Aaron Letterly and Jeff Key, providing new figures based on ABI data and a description of a post-processing procedure to convert the output to from image coordinates to latitude/longitude space. Version 2.3 was created by Aaron Letterly, Jeff Key, and Yinghui Liu, converting the previous, GOES-R-specific document to an Enterprise version.

1.6 Acknowledgements

The original ice motion code was provided by Chuck Fowler, Colorado Center for Astrodynamics Research, University of Colorado-Boulder. Section 3.4.1 was contributed by Walt Meier, National Snow and Ice Data Center.

2 OBSERVING SYSTEM OVERVIEW

This section describes the products generated by the ABI Ice Motion (AIM) algorithm and the sensor requirements.

2.1 Instrument Characteristics

The ABI onboard the future GOES-R has a wide range of applications in weather, oceanographic, climate, and environmental studies. ABI has 16 spectral bands, with 2 visible bands, 5 near-infrared bands, and 9 infrared bands. The spatial resolution of ABI will be nominally 2 km for the infrared bands, 1 km for 0.47, 0.86, and 1.61 μm bands, and 0.5 km for the 0.64 μm visible band. ABI will scan the full disk every 15 minutes, plus continental United States 3 times, plus a selectable 1000 km × 1000 km area every 30 s. ABI can also be programmed to scan the full disk every 5 minutes. Compared to the current GOES imager, ABI offers more spectral bands and higher spatial resolution. Especially, the newly added bands at 1.61 μm, and higher spatial resolution at 0.64 μm allow for a better detection and monitoring of surface snow and ice (Schmit et al., 2005).

The ice motion is determined for each pixel observed by the ABI. In the current version of algorithm, the infrared band with wavelength 11.2 μm is used. The visible band at a wavelength of 0.64 μm is being tested for its very high spatial resolution. Table 1 lists the ABI bands and which are used in this algorithm.

The VIIRS onboard the S-NPP and the JPSS satellites has 22 spectral bands covering wavelengths from 0.4 to 11.8 μm (Table 2). The S-NPP was launched on October 28, 2011; the first JPSS satellite, JPSS-1, was launched on November 18, 2017. Among the 22 bands, there are 5 high resolution imagery bands (I-bands, 375 m spatial resolution at nadir), 16 moderate resolution bands (M-bands, 750 m spatial resolution at nadir), and one Day/Night Band (DNB, 750 m spatial resolution). The VIIRS swath width is 3000 km. Table 2 lists the VIIRS bands and which are used in this algorithm.

The METimage onboard the second generation of Metop satellites (Metop-SG) covers a broad spectral range in 20 spectral bands and is expected to have comparable performance with respect to VIIRS on NOAA satellites. METimage channel VII-12, with a central wavelength of 0.668 μm, is similar to ABI Channel 2 from which ice motion is already derived. Cloud detection using METimage channel VII-37 (central wavelength 10.69 μm) will be done similarly to ABI channel 14 cloud detection. Table 3 lists the METimage bands and which are used in this algorithm.

AMSR2 is a microwave instrument that was launched in 2012 on board GCOM-W1 satellite. Now that GCOM-W1 is part of the "A-train" constellation along with Aqua and AMSR-E and AMSR2 have the same center frequencies and corresponding bandwidths, AMSR2 is considered as the successor to AMSR-E. AMSR-E is a passive microwave radiometer sensing microwave radiation at 6 frequencies ranging from 6.9 to 89.0 GHz with fields of view from approximately 5 to 50 km. AMSR-E onboard the polar-orbiting satellite (Aqua) operationally provided sea ice properties until it failed in regular scanning due to an antenna problem in October 2011. However, AMSR2 has several enhancements: larger main reflector, additional 7.3 GHz channels, an improved calibration system, and improved spatial resolution (Table 4).

Table 1. *Summary of the Current ABI Band Numbers and Wavelengths.*

Band Number	*Wavelength (μm)*	*Used in AIM*
1	0.47	
2	0.64	✓
3	0.86	
4	1.38	
5	1.61	
6	2.26	
7	3.9	
8	6.15	
9	7.0	
10	7.4	
11	8.5	
12	9.7	
13	10.35	
14	11.2	✓
15	12.3	
16	13.3	

Table 2. *VIIRS band numbers and wavelengths.*

Band Number	***Wavelength (μm)***	***Subsatellite Field of View (km)***	***Used in AIM***
M1	0.411	0.750	
M2	0.444	0.750	
M3	0.486	0.750	
M4	0.551	0.750	
I1	0.639	0.375	
M5	0.672	0.750	✓
M6	0.745	0.750	
I2	0.862	0.375	
M7	0.862	0.750	
M8	1.238	0.750	
M9	1.375	0.750	
I3	1.602	0.375	
M10	1.602	0.750	
M11	2.257	0.750	
I4	3.753	0.375	
M12	3.697	0.750	
M13	4.067	0.750	
M14	8.578	0.750	
M15	10.729	0.750	✓
I5	11.469	0.375	✓
M16	11.845	0.750	
DNB	0.7	0.750	✓

Table 3. *METimage (VII) channel numbers and wavelengths.*

Channel Number	***Wavelength (μm)***	***Bandwidth ((μm)***	***Used in AIM***
VII-4	0.443	0.03	
VII-8	0.555	0.02	
VII-12	0.670	0.02	✓
VII-15	0.752	0.01	
VII-16	0.763	0.01	

VII-17	0.865	0.02	
VII-20	0.914	0.02	
VII-22	1.240	0.02	
VII-23	1.375	0.04	
VII-24	1.630	0.02	
VII-25	2.250	0.05	
VII-26	3.740	0.18	
VII-28	3.959	0.06	
VII-30	4.050	0.06	
VII-33	6.735	0.37	
VII-34	7.325	0.29	
VII-35	8.540	0.29	
VII-37	10.690	0.50	✓
VII-39	12.020	0.50	
VII-40	13.345	0.31	

***Table 4**. Comparison of AMSR2, AMSR-E, and MWI features.*

AMSR2	**Center Freq (GHz)**	**6.9/7.3**	**10.7**	**18.7**	**23.8**	**36.5**	**89.0**
	Band Width (MHz)	350	100	200	400	1000	3000
	IFOV (km x km)	35x62	24x42	14x22	15x26	7x12	3x5
AMSR-E	**Center Freq (GHz)**	**6.9**	**10.7**	**18.7**	**23.8**	**36.5**	**89.0**
	Band Width (MHz)	350	100	200	400	1000	3000
	IFOV (km x km)	43x75	29x51	16x27	18x32	8x14	4x6
MWI	**Center Freq (GHz)**			**18.7**	**23.8**	**31.4**	**89.0**
	Band Width (MHz)			200	400	1000	4000
	IFOV (km)			50	50	30	10

The algorithm relies on utilizing the cross correlations between sets of pixels between image pairs to determine motion. This method, typically referred to as a Maximum Cross-Correlation (MCC) procedure, is widely used, including applications to Advanced Very High Resolution Radiometer (AVHRR), synthetic-aperture-radar (SAR) data, passive microwave and scatterometer data, and has been adapted for use in the ABI. A spatial coherence filter, a displacement filter, and threshold of the correlation coefficients are also applied to distinguish realistic ice motion vectors from cloud motions.

2.2 Products Generated

The ice motion algorithm is responsible for determining the motion of ice for all clear and non-land ABI pixels with ice cover. It operates over ocean and large lakes (e.g., the Great Lakes). In terms of the MRD, it is responsible directly for the movement within the Cryosphere category. The current ice motion design calls for a u and v movement in pixel space. The required product Function and Performance Specification (F&PS) for ice motion is listed in Table 5.

Table 5. *Product Function and Performance Specification for sea and lake ice motion.*

Name	Sea & Lake Ice Motion
User and Priority	GOES-R
Geographic Coverage (G, H, C, M)	FD: Sea ice covered waters in N & S Hemisphere
Vertical Resolution	N/A
Horizontal Resolution	15 km
Mapping Accuracy	7.5 km
Measurement Range	Direction: 0 to 360°, and displacement 0 to 0.6 m/s
Measurement Accuracy	Direction: 22.5°, Speed 3 km/day
Product Refresh Rate/Coverage Time	6 hr
Vendor Allocated Ground	9716 sec
Product Measurement Precision	Direction: 30°, Speed 3 km/day

3 ALGORITHM DESCRIPTION

Complete description of the algorithm is provided in this section. An overview, processing outline, and a more in-depth description of the basis for the algorithm is provided.

3.1 Algorithm Overview

The ABI ice motion algorithm is based upon the methodology used by the National Snow and Ice Data Center's Polar Pathfinder Daily 25 km EASE-Grid Sea Ice Motion Vectors for gathering ice motion vectors from the AVHRR instrument (Fowler, 2003). The ice motion output is in x and y coordinates of a standardized global grid, with the u and v components of motion. This algorithm may also be applied to other satellite data, notably passive microwave. Presently, the algorithm described here is being implemented in daily (non-operational) research using data from Visible Infrared Imaging Radiometer Suite (VIIRS) M15 band (11 μm) as well as the Advanced Microwave Scanning Radiometer 2 (AMSR2). Comparisons between VIIRS ice motion and ice motion from other entities show good agreement. It is expected that this will become NOAA's "Enterprise" algorithm for ice motion.

3.2 Processing Outline

The processing outline of the AIM is summarized as follows:

- Process full image of 11 μm Brightness Temperature (BT).
- Load 11 μm image from 24 hours prior.
- Make common cloud mask that is the union of the current cloud mask and the one from 24 hours prior. Re-map to common grid.
- Run the ice motion program.
- Determine the motion vectors based on the ice cover mask
- Run the vector filtering program.
    - This outputs vectors of points and motion in image space
- Run the post-processing program that converts the ice motion vectors from image coordinates to latitude/longitude space.

A flow chart of the processing of the AIM is shown in Figure 1.

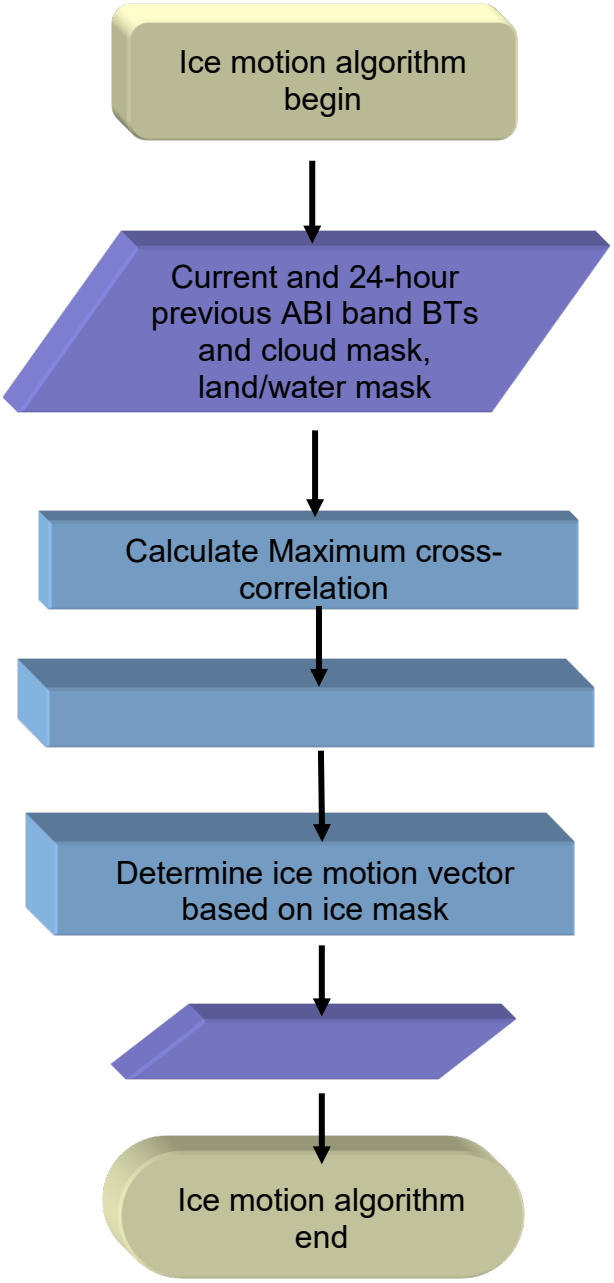

ABI Band Used:
Band No 2
Band No 14

Algorithm Dependencies:
Cloud mask
Ice mask

Ancillary Data Dependencies:
Land/water mask.

Products Generated:
Ice motion vector and associated quality flags.

Figure 1. *High Level Flowchart of the ice motion algorithm illustrates the main processing sections.*

3.3 Algorithm Input

This section describes the input needed to process the AIM. The AIM requires knowledge of the surrounding pixels. In its current operation, we run the AIM on all pixels from both the current and previous images. The AIM is not designed to run with information from only one pixel or just one image

3.3.1 Primary Sensor Data

The list below contains the primary sensor data used by the AIM for both ABI and VIIRS. By primary sensor data, we mean information that is derived solely from the ABI observations and geo-location information. Correlations are calculated between BTs (or reflectance) inside different sub-windows in two images.

- Current calibrated 11 μm BTs (0.64 μm normalized reflectance)
- Calibrated 11 μm BTs (0.64 μm normalized reflectance) from 24 hours prior.

Visible data, e.g., 0.64 μm reflectance, normalized by cosine of solar zenith angle, could be used instead. Retrievals would, of course, be limited to the sunlit portion of the day and year.

Proxy data from EUMETSAT (given in radiances) was converted to visible reflectances and brightness temperatures for band 12, which has similar central wavelength characteristics to the 0.64 μm channel on ABI.

The rest of this document therefore assumes that the 11 μm BT band is used.

3.3.2 Static Ancillary Data

3.3.2.1 *Static Ancillary Data*

The following data lists and briefly describes the ancillary data required to run the AIM. Static ancillary data represents data that requires information not included in the ABI observations or geo-location data and does not change with each image. The only static dataset that is useful to the AIM is the pixel level land/water mask, which comes from the NASA 1 km global land cover. This can be an output from the AIT Framework data structures.

3.3.2.2 Dynamic Ancillary Data

The following lists and briefly describes the dynamic ancillary data required to run the AIM. Dynamic data represents data that changes with each image and is not included in the ABI observations or geo-location data. The AIM requires two sets of dynamic ancillary data. First are the current image pixel level GOES-R ABI cloud and ice masks, and second are the cloud and ice masks from 24 hours previous. These are necessary to provide an accurate idea of where clear sky and ice pixels are located.

3.4 Theoretical Description

Ice motion detection is the process of determining the movement of pixels that are ice pixels. It always involves assumptions of the radiometric characteristics of ice,

particularly those that relate to the BTs in the 11 μm band, and reflectance in the 0.64 μm band. In the AIM, a small target area in one image is correlated with many areas of the same size in a search region of the second image. The displacement of the ice is then defined by the location in the second image where the correlation coefficient is the highest with the small target area in the first image. This process makes the basic assumptions that the sea-ice cover can be treated as a solid, with the ice movement only a translation of this solid plane (e.g., ignoring deformation and rotation of the ice), and the radiative property of the pixels does not change significantly over the 24 hour period. These assumptions are generally valid over short distances away from ice edges such as the marginal ice zone where the ice is less constrained. However, radiative properties can change during onset of melt, snowfall, etc. (Maslanik et al., 1998). Two extra filters are applied to the output ice motion vectors to obtain less noisy and more useful results, as described later.

The selection of the sizes of the target area and search windows in the images depends upon several factors. The size of the target window cannot be so large as to negate this solid-plane assumption, but the window size must be large enough so that the correlation still has some statistical significance. Also, the size of the search window is in part dependent upon the expected displacement of the ice. In the current algorithm, a 15-pixel by 15-pixel square search window is selected. The size of the search window can be easily changed in an input parameter file.

3.4.1 Ice Motion Physics

The motion of an individual ice floe is governed by the balance of the forces that act on that floe. This can be expressed using what is often called the momentum equation, simply Newton's third law of motion:

$$\sum F = ma = m\frac{Du}{Dt}$$

here m is the mass of the ice. We usually express the forces in terms of stress (force per unit area), so the mass will be in mass per unit area, or the ice density multiplies by its thickness (H), The external stresses acting on the ice floe are the wind stress, τ_a, the water stress, τ_w, the apparent force due to Coriolis, τ_c, the force due the tilt of the water surface, τ_t, and the internal ice stress, τ_i. Therefore,

$$m\frac{Du}{Dt} = \tau_a + \tau_w + \tau_c + \tau_t + \tau_i$$

Which terms are most important depends on the scales of interest. More details can be found in Maslanik et al. (1998) and Thorndike and Colony (1982). Theoretically, ice motion vectors can be derived by solving the above non-linear equation. In satellite remote sensing applications, correlation coefficient analysis between two satellite images is often used to derive ice motion vectors. Details are explained in the next section.

3.4.2 Mathematical Description

Mathematically, the AIM is fairly simple, the core is the correlation coefficient between BTs (reflectance) in two satellite images (Emery et al. 1991). The correlation coefficient is calculated based on the linear regression theory. More specifically, for a n-pixel by n-pixel square sub window, window A, in one satellite image, cross-correlations are calculated between 11 μm BTs (0.64 μm reflectance) of all clear pixels over water in window A and 11 μm BTs (0.64 μm reflectance) of all clear pixels over water in $(2d+1)^2$ square sub windows with the same window size in the other image surrounding Window A, where d is the maximum allowed displacement of the sub-window in pixel space. The search begins from left to right of 2d+1 columns for each of 2d+1 rows. Then the sub window with the maximum cross coefficient with Window A can be found, called Window B. The displacement in pixel space between the centers of Window A and B is the displacement of the ice floe. Ice motion vector can be determined by the ratio of this displacement in physical space (by multiplying the pixel size) to the time interval of these two images. Same ice motion vectors are assigned to all the pixels with ice covered in window A. This method, typically referred to as a Maximum Cross-Correlation procedure, is widely used, including routine applications to AVHRR, SAR, passive microwave and scatterometer data. Since the number of correlations done in the MCC process is $(2d+1)^2$, computation time increases exponentially as the value for d (the maximum ice movement distance) increases. In the current algorithm, pixel size n is 15, and maximum displacement, d, is being tested from 5 to 25 pixels.

The correlation value, is simply the result of simple division, where the numerator and denominator are as follows:

$$\text{num} = n * \sigma_{i1i2} - \sigma_{i1} * \sigma_{i1}$$

$$\text{denom} = \sqrt{((n * \sigma_{i11} - \sigma_{i1} * \sigma_{i1}) * (n * \sigma_{i22} - \sigma_{i2} * \sigma_{i2}))}$$

Where n is the total number of pixels in the search box, σ_{i1} is the sum of all the pixels in the search box for the first image, σ_{i2} is the sum of all the pixels in the search box for the second image, σ_{i11} is the sum of all the squares of the pixels in the search box for the first image, σ_{i22} is the sum of all the squares of the pixels in the search box for the second image, σ_{i1i2} is the sum of all pixels in the search box for the first image times the corresponding pixel in the second image.

Filtering is done on the resulting vectors from the initial calculation of the motion and is done in three steps. First is that all vectors with correlation values below 0.5 are eliminated. This is to ensure only highly correlated values are output. The second step is that vectors are kept if at least a certain number (3) of (total 9) neighboring vectors are within a certain similar pixel displacement (1 pixel) in both u and v directions. Finally, data with speeds greater than 60 cm/s are eliminated. This ensures that there all fast-moving pixels (which are likely motions of cloud targets) and non-moving pixels are not output.

3.4.3 Algorithm Output

The final outputs of this algorithm are ice motion in u and v motion in grid space. The ice motion values can range between 0 ~ 60.0 cm/s, which depends on the pixel size of the sub window and the maximum allowable displacement. The values for the correlation values have no dimensions but have a value between 0.0 and 1.0. For geostationary satellite observations like GOES-R ABI, with the increase of the latitude, the pixel size of Instantaneous Field of Views (IFOV) increases among other changes, which affects the derivation of the ice motion vectors and their qualities, e.g. resolution. The maximum latitude of the ice motion vector is the latitude with 67 degrees local zenith angle, which is correspondent to latitude less than 60 degrees North. For pixel size 2 km under the nadir view, the resolution near the Arctic, 60 degrees North, is around 5 km for 11 μm band, and the resolution over the Great Lakes, 45 degrees North, is around 3 km. Better image resolution for the visible band, 0.5 km at 0.64 μm band, results in resolution around 0.75 km over the Great Lakes and 1.25 km over 60 degree North Latitude, which makes the quality of the ice motion vectors much better. In this regard, observations with higher spatial resolution, like 0.5 km spatial resolution for ABI 0.64 μm band, improve the quality of the output ice motion vector. The quality flag information of the product is listed in Table 6, with metadata information followed.

Table 6. *Sea and Lake Ice Motion Quality Information (1 byte).*

Byte	Bit	Quality Flag Name	Description	Meaning
1	0 1	QC_IceMotion	Ice motion quality	00- Good 01- Uncertain 10- Non-retrieval 11 – Bad retrieval
	2	QC_CLDMASK	Clear from both current and previous images?	0-yes 1-no
	3	QC_LandMask	Water from both current and previous images?	0-yes 1-no
	4	QC_ICEMASK	Ice covered from current or previous images?	0-yes 1-no
	5	QC_OBS_PREV	Valid Observation from previous image?	0-yes 1-no
	6	QC_OBS_CURR	Valid Observation from current image?	0-yes 1-no

The ice motion product is a Full Disk product with a 3-hour refresh rate. The ice motion algorithm needs to run on every Full Disk image during the 3-hour period with image from 24-hour prior. Ice motion at each pixel in the Full Disk ice motion product at the end of every 3-hour period comes from the available ice motion output at the same

location in the closest image in time during that 3-hour period. The horizontal resolution of ice motion is ~5 km for Full Disk. The output of ice motion at the ABI resolution needs to be interpolated linearly to the required spatial resolution.

Common metadata for all data products:

- DateTime (swath beginning and swath end)
- Bounding Box
  - Product resolution (nominal and/or at nadir)
  - Number of rows, and number of columns
  - Bytes per pixel
  - Data type
  - Byte order information
  - Location of box relative to nadir (pixel space)
- Product Name
- Product units
- Ancillary data to produce product (including product precedence and interval between datasets is applicable)
  - Version Number
  - Origin
  - Name
- Satellite
- Instrument
- Altitude
- Nadir pixel in the fixed grid
- Attitude
- Latitude, longitude
- Grid projection
- Type of scan
- Product version number
- Data compression type
- Location of production
- Citations to documents
- Contact information

Metadata specific to the Sea and Lake Ice Motion product with quality information:

- Pixel size of sub-window
- Maximum Local zenith angle limit
- Threshold of minimum clear-sky water surface percentage in a sub-window
- Maximum correlation coefficient threshold
- Threshold of maximum u and v-component
- Total number of pixels with ice cover
- Total number of valid ice motion retrievals
- Total percentage of valid ice motion retrievals to all pixels with ice cover
- Total pixels numbers and percentage of terminator pixels (Non-retrievable and Bad data)
- Mean, Min, Max, and standard deviation of the speed of the ice motion retrievals

3.4.4 Post-Processing of AIM Output

A post-processing procedure is now employed to convert the original output, which consists primarily of ice motion vectors, from image coordinates to latititude/longitude ("lat/lon") space. It reads the filtered output of the ice motion. The procedure computes the latitude and longitude of the starting and ending points of each ice motion vector, then recomputes the u- and v- components of the motion in lat/lon coordinates. It then writes the additional information and the original information to a new file.

The program uses the following input files:

- The filename of the original AIM output.
- The filenames of the latitude and longitude files, which are floating point, two-dimensional arrays corresponding to the images used in the AIM algorithm.
- The parameter file, which specifies the time difference between the two images and is also used as input into the AIM program.

The program produces the following output file:

First line: The two image file names used in tracking. This is the same as the original AIM output.

Second line: The number of vectors in x and y directions, the image size x and y, and a constant to convert the velocities back to pixel displacements. This is the same as the original AIM output.

The subsequent lines will correspond to individual motion vectors and will have the following information in this order:

- X-location of the vector
- Y-location of the vector
- U-velocity (in centimeters/second) in grid (x,y) space
- V-velocity (in centimeters/second) in grid (x,y) space
- Correlation for the tracked feature
- Latitude of the starting point of the motion vector
- Longitude of the starting point of the motion vector
- Latitude of the end point of the motion vector
- Longitude of the end point of the motion vector
- U-component of the motion calculated in lat/lon space (positive U means movement toward the East and a positive V is movement toward the North)
- V-Component of the motion calculated in lat/lon space
- Speed (km/day)
- Direction from which the motion is coming (in degrees)

4 Test Data Sets and Validations

4.1 Tests with MODIS

Initially, the AIM was tested in near real time at the Moderate Resolution Imaging Spectroradiometer (MODIS) Direct Broadcast site at Tromsø, Norway, using data from the Integrated Program Office's direct broadcast system, operated by Kongsberg Satellite Services (KSAT). This data was compared to buoy measurements from the International Arctic Buoy Program, operated by the University of Washington, with funding from the U.S. Interagency Buoy Program (USIABP) through the National Ice Center (NIC). MODIS is used because of the coverage over the regions with buoy measurements as well as coverage of moving ice on a nearly daily basis. The direct broadcast system is useful as it provides a platform for near real-time processing testing. Data is remapped to a standard grid, much like what is proposed for ABI. In addition, the location of the direct broadcast systems in the polar regions allows for near complete coverage of the Arctic and Antarctic testing in near real time. An example is given in Figure 2.

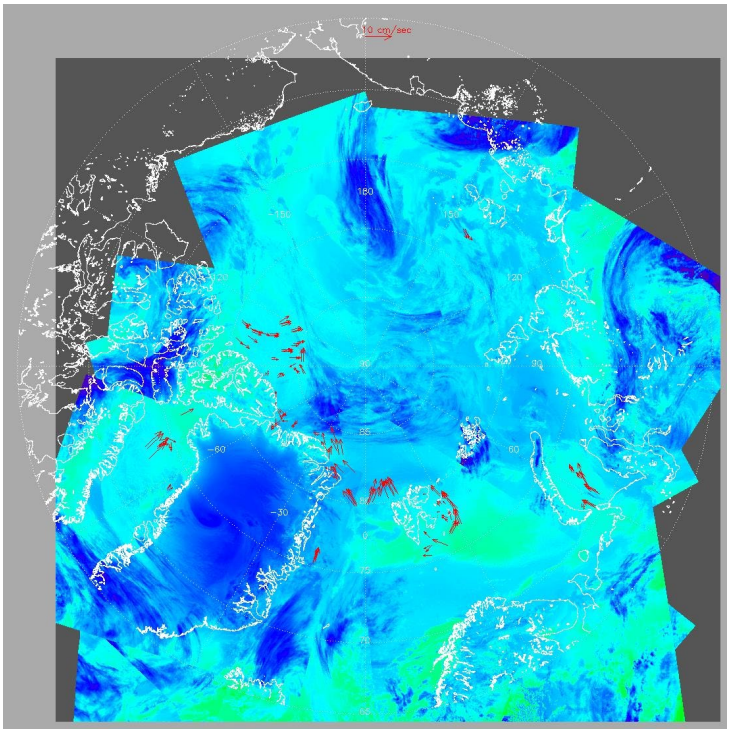

Figure 2. *Composite of 11 µm brightness temperature and ice motion vectors from MODIS, using data from Tromso, Norway, for May 20, 2008*

In addition to generating ice motion from ABI, the algorithm is also being run routinely with Visible Infrared Imaging Radiometer Suite (VIIRS) and Advanced Microwave Scanning Radiometer 2 (AMSR2) data. Examples are available at http://stratus.ssec.wisc.edu/gcom/rtproducts/.

4.2 Tests with ABI

A second study was performed for February 14, 2018, utilizing GOES-16 ABI Channel 2 data over the contiguous United States. Using the high-resolution (0.5 km) data from the ABI "CONUS scan" is an example of the capabilities of the ice motion code to determine small-scale ice motion with high temporal resolution. The cloud-free day over the central/eastern Great Lakes showed apparent ice motion between 13:00 and 20:00 local time. Using subsets of two ABI Channel 2 images from 13:42 and 18:27 local time with cloud-free views of Lake Michigan and Lake Huron, we calculated speed and direction of the ice floes. Evaluation of the ice motion was performed by setting the 15-by-15 cell target box to a 15 cell scan range, which assumes that features did not move more than 15 km in the five-hour period. This test also assumes that ice features greater than 15-by-15 cells in size will not be effectively tracked, which is why larger ice floes in southern Lake Michigan do not show consistent motion.

No cloud mask or ice mask was used during the AIM routine or the filtering step. Figure 3 gives an example from the test case period, where vectors with correlation coefficients of 0.75 or higher are spatially averaged over every 10-by-10 pixel cell.

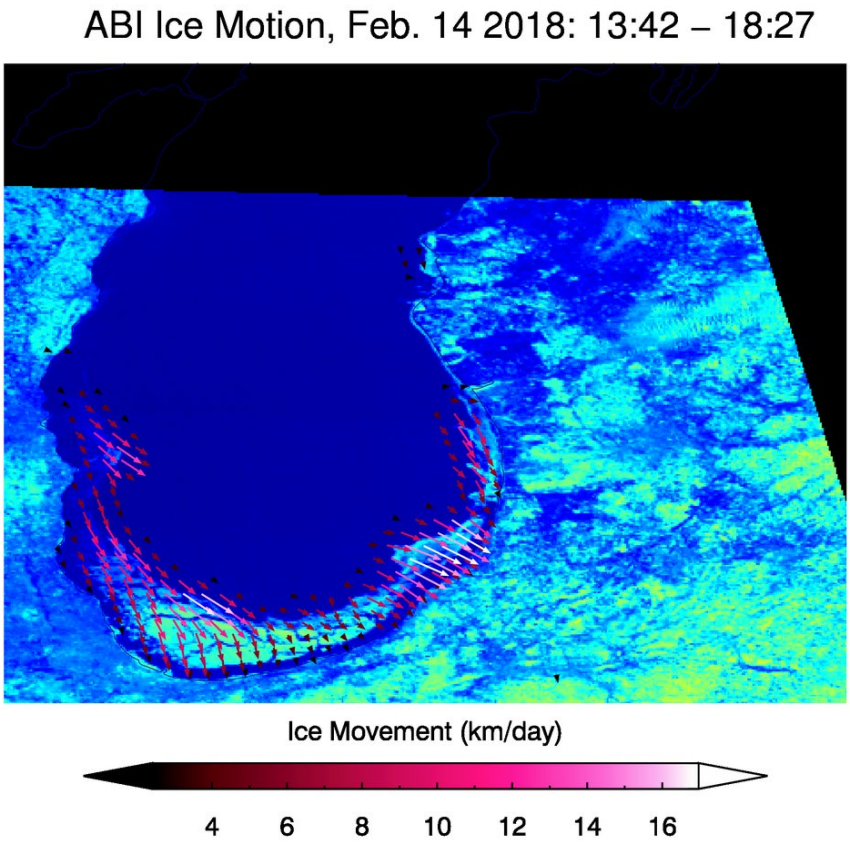

Figure 3. *Subset of 0.64 µm brightness temperatures and ice motion vectors from GOES-16 ABI, using data between 13:00 and 18:00 for February 14, 2018.*

4.3 Tests with AMSR2

Passive microwave radiation input data from the AMSR2 89 GHz channel have provided a consistent and high-quality source of daily ice motion estimations. Large-scale ice motion patterns over the entire Arctic can be determined without gaps due to cloud cover, unlike ice motion from VIIRS and ABI. The nominal spatial resolution of the dataset (6.25km) is regrid into a 2km EASE-Grid, which is still significantly lower than VIIRS I-band resolution (375m), but still capable of resolving ice motion at useful spatial scales. First, composite hemispheric images for the Arctic and Antarctic are put together from multiple swaths over the course of a 24-hour period. Next, the daily composite image pair from two separate days are used as input into the ice motion algorithm. This process is similar to the other applications of this algorithm except that a cloud mask is not needed as an input. Ice motion output from the input data is produced daily for both the Arctic and Antarctic, and is only unreliable during high summer, when high emissivity from liquid water melt ponds interferes with the emissivity from the surrounding sea ice. Using two 89 GHz images from AMSR2, the ice motion output shown below in Figure 4 was produced for the period of March 12-13, 2020 and is focused on the Alaska. Vectors in Figure 4 are drawn every 30 km.

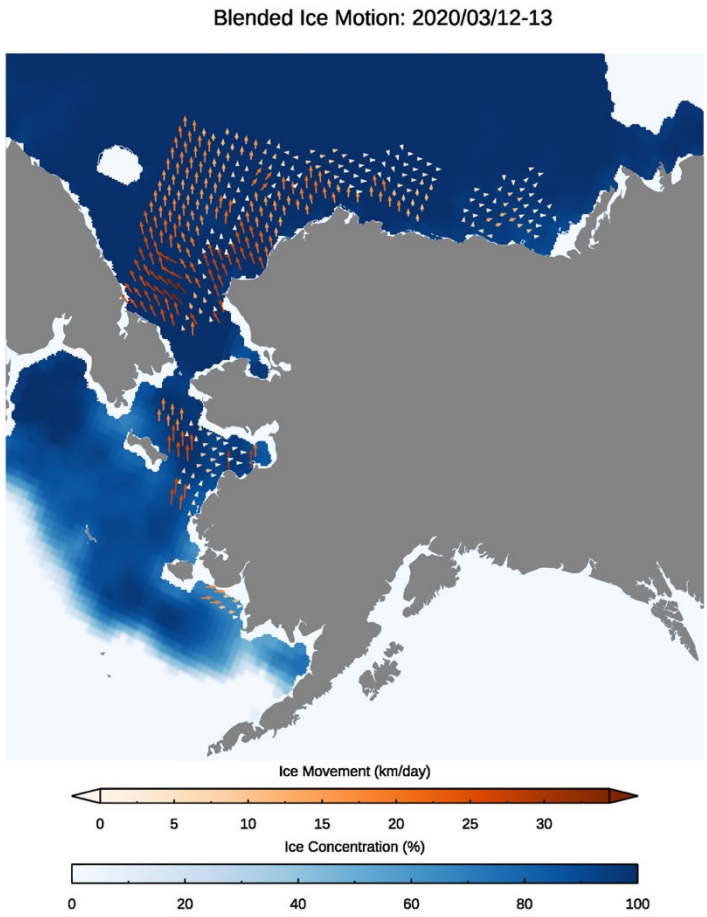

Figure 4. *Blended AMSR2 89 GHz and VIIRS ice motion vectors centered over Alaska during March 12-13, 2020.*

4.4 Tests with VIIRS

Input data from VIIRS 375m resolution I05 band (10.5 – 12.4 µm) are used to generate high resolution sea ice motion in cloud-free areas using the same algorithm that produces ABI ice motion. At the resolution of VIIRS I-bands, the motions of individual sea ice floes may be observed and compared to other high-resolution sea ice motion data sources such as those from Sentinel-2 SAR. Due to ubiquitous Arctic cloud cover, 24-hour imagery composites are not generated, and ice motion is determined based on spatially overlapping swaths that are approximately 24 hours apart. This imagery is regrid onto a 500m EASE grid. Ice motion from the VIIRS M15 band as well as the Day/Night Band is also produced on a 1km grid. Though not as spatially continuous as sea ice motion derived from passive microwave, the algorithm produces sea ice motion in cloud-free areas that has matched closely with buoy data when compared. The sea ice motion field shown in Figure 5 was estimated using two VIIRS I05 band images north of the Svalbard archipelago. Vectors in Figure 5 were drawn every 25 km.

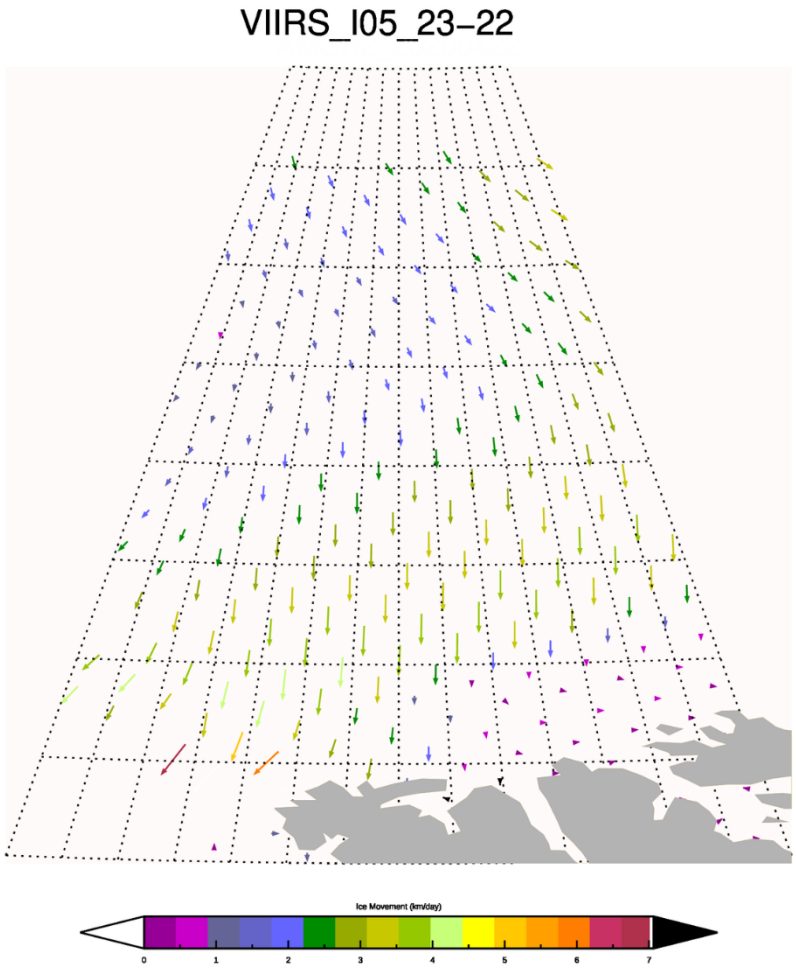

Figure 5. VIIRS I05 Band ice motion vectors shown north of the Svalbard archipelago during May 22-23, 2020.

4.5 Output from Simulated Input Data Sets

4.5.1 Precision and Accuracy Estimates

A test study was taken from May 4-9, 2008, and February 18-20, 2008 utilizing near real-time data from the MODIS Direct Broadcast site at Tromsø, Norway. Buoy measurements provide latitude, longitude and UTC every 45 minutes to 1 hour. Using these observations, we can calculate speed and direction of the buoy. Evaluation of the buoy data and data measured from the AIM was performed by assuming that motion is within 50km of the buoy data. There are a total of 1654 comparisons for this time period. Figure 6 is an example from the test case period.

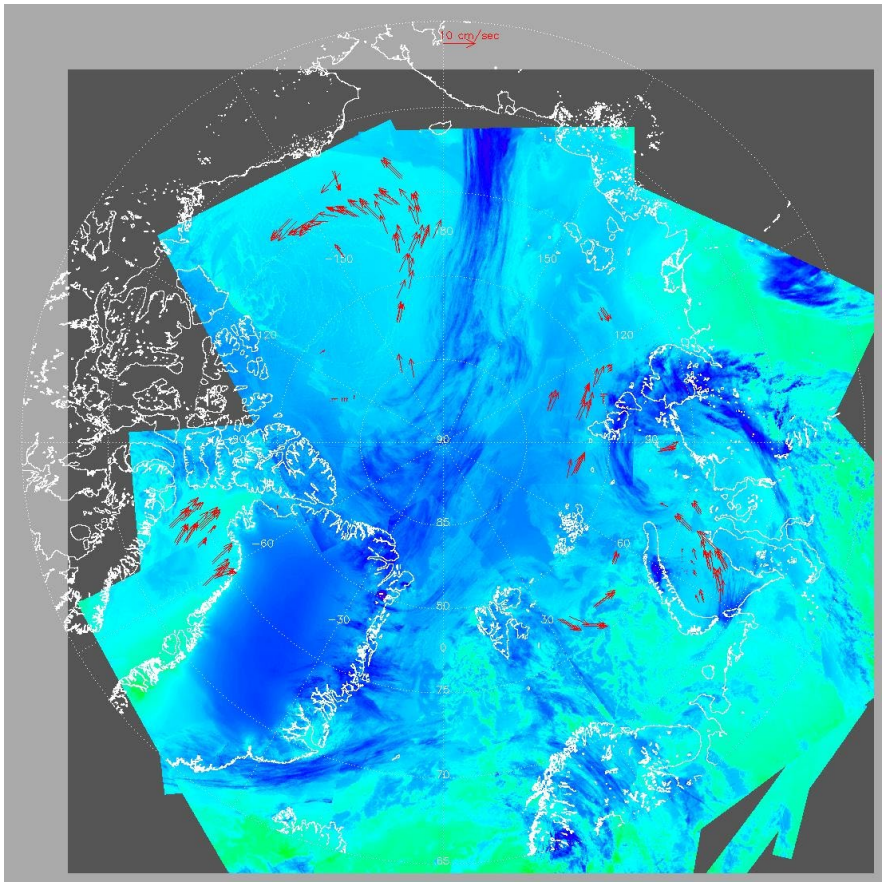

Figure 6. *Composite of 11 µm brightness temperature and ice motion vectors from MODIS, using data from Tromso, Norway, for May 8, 2008*

4.5.2 Error Budget

The average speed difference for the case study time period was approximately 0.25 cm/s with standard deviation 3.4 cm/s, and had an average directional difference of 2.9 degree,

with standard deviation 30.0 degree. The maximum speed difference was approximately 6 cm/s and the maximum absolute directional difference was approximately 50 degrees (Figure 7, Table 7). These large differences are likely due to the fact that none of the ice motion vectors were closer than about 20 km. Based on these results, both accuracy and precision of this algorithm meets the F&PS requirements. Routine validation of ice motion vectors over the Arctic Ocean will continue. Further validation over mid-latitude will be carried out when in situ observations become available.

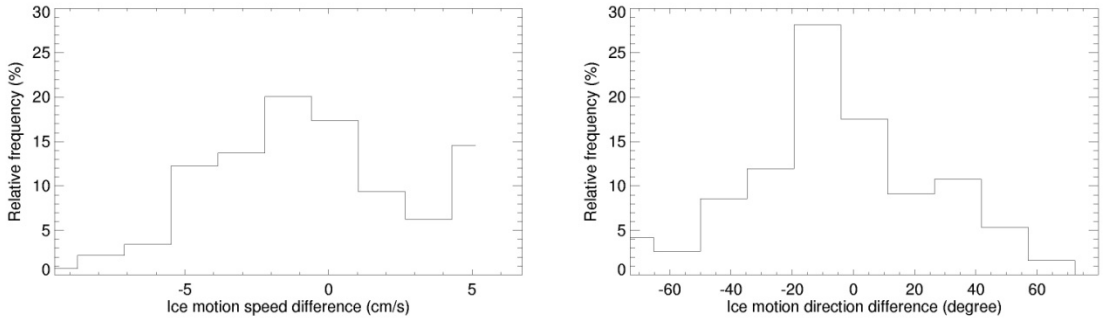

Figure 7. *Frequency distributions of ice motion speed (left) and direction (right) difference between MODIS retrieved and from buoy data.*

Table 7. *Error analysis of retrieved ice motion direction and speed.*

Ice motion product performance by comparison with buoy data 1654 pairs	Mean bias	Standard Deviation
Ice motion speed	0.25 cm/s	3.4 cm/s
Ice motion speed required accuracy and precision	3.5 cm/s (3 km/day)	3.5 cm/s (3 km/day)
Ice motion direction	2.9 degree	30.0 degree
Ice motion direction required accuracy and precision	22.5 degree	30.0 degree

4.6 Output from Simulated EPS-SG METimage Input

A test of ice motion-tracking capabilities from the EPS-SG METimage proxy data from EUMETSAT was performed in December 2019 in preparation for the EPS-SG ice products review. Radiance, geolocation, and ancillary data were provided and were used to produce input for the ice motion algorithm. Radiances were converted to visible reflectances as well as brightness temperatures before processing.

Since ice motion requires multiple overlapping swaths and the available proxy data was limited, data over Antarctica from September 12, 2007 were used. These data were only 100 minutes apart (9:18 a.m. to 10:41 a.m.), though many other tests referred to within this ATBD use brightness temperature input approximately 24 hours apart. As a result, ice motion from this test is far more constrained in comparison to 24-hour tests performed with other data. Figure 6 shows the 100-minute ice motion output (top) from the METimage proxy data. Vectors at the edge of the Ronne Ice Shelf show ice motion moving out towards the Weddell Sea from the Antarctic Peninsula. Further into the Weddell Sea, ice motion is determined to be towards more northerly latitudes and eastward. This general ice motion pattern is matched by the 1000 millibar (mb) wind field (bottom) approximately thirteen hours later on 00:00Z, September 13.

In order to determine the general pattern of ice motion, a density-based clustering routine uses 50-pixel square boxes to produce Figure 8, shown below. The clustering routine takes into consideration over 36,500 ice motion vectors created by the ice motion algorithm. Inhomogeneity in the ice motion vectors are likely due to cloud interference, gaps in data due to remapping, or both. Wind vectors are taken from the Plymouth State Weather Center upper-level wind archives (https://vortex.plymouth.edu/).

In addition, Figure 9 shows sea ice motion from METimage proxy data during January 03, 2020 over the Arctic. In order to show detail, the spatial domain of Figure 9 has been reduced to show sea ice motion vectors off the coast of Disko Island (West Greenland) over a 105-minute interval. Since no cloud mask was available for the proxy data, a filter removing any sea ice motion over 5 km/hr was used to filter out fast-moving clouds. It is possible, however, that the output contains some artifacts due to cloud contamination.

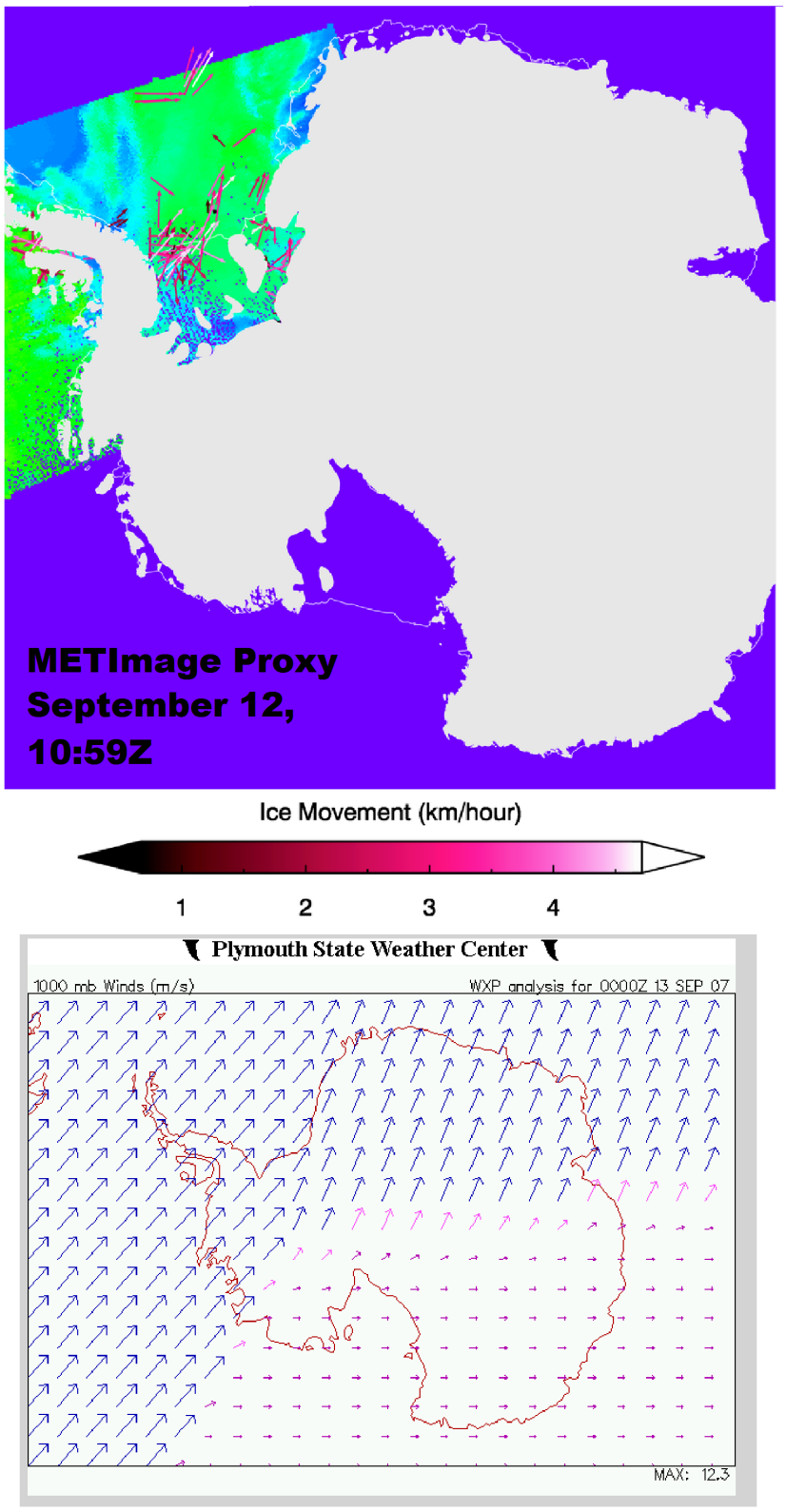

Figure 8. *Ice motion output from METimage proxy data (top) at 10:59Z, Sept. 12, 2007. Surface wind field (00:00Z) shown bottom.*

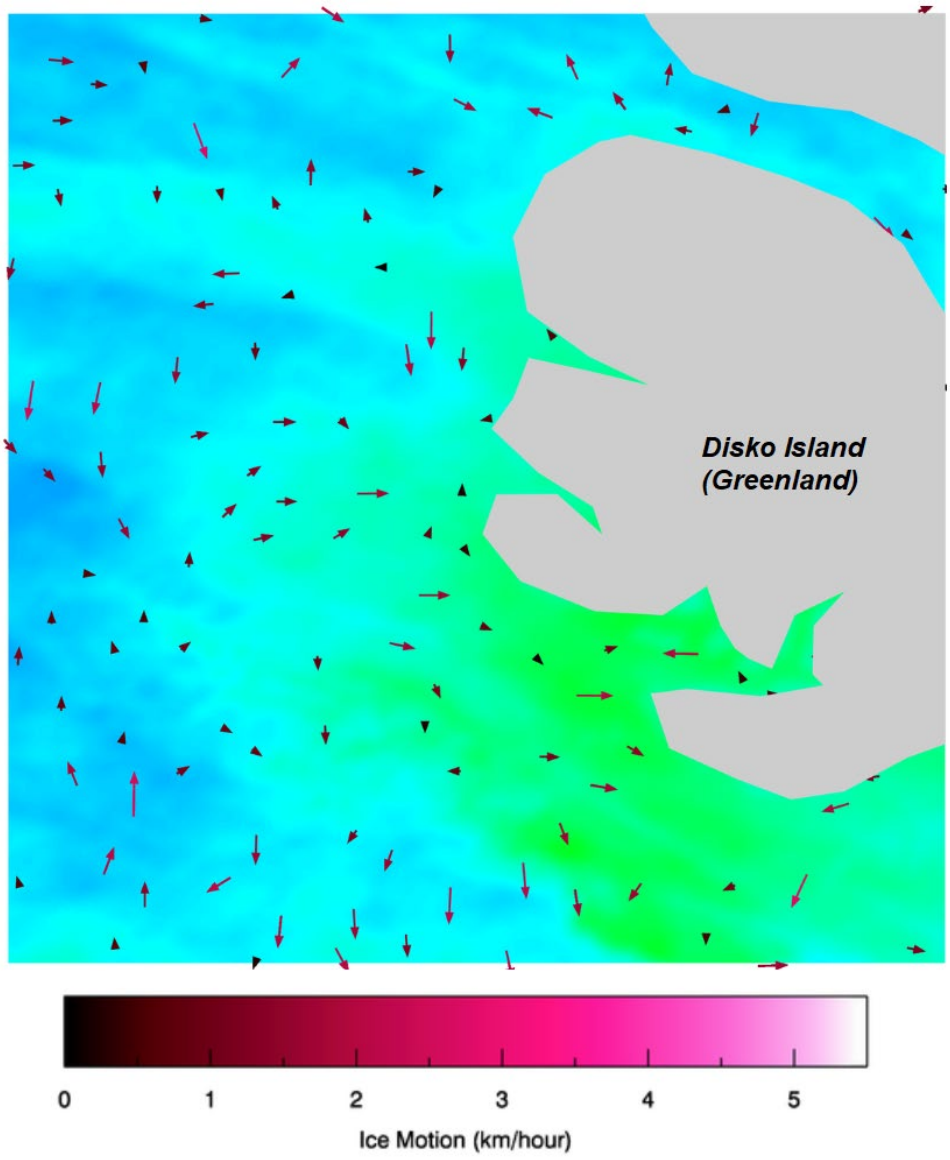

Figure 9. *Ice motion output from METimage proxy data from 9:05 p.m. – 10:45 p.m., January 3, 2020 near Disko Island (West Greenland).*

5 PRACTICAL CONSIDERATIONS

5.1 Numerical Computation Considerations

All input image data, e.g., 11 μm BTs (0.64 μm reflectance), need to be remapped to common grid, because two images with the same projection are required. One advantage of ice motion retrieval using GOES-R ABI is that such re-mapping is not necessary, since all ABI images are with the same map projection, assume geo-registration of GOES-R ABI is accurate. Computation time of the MCC method increases linearly to the square of maximum allowable displacement of the sub-window in pixel space, as described in section 4.4.2. This should be taken into account when changing the maximum allowable displacement is considered.

5.2 Programming and Procedural Considerations

Because the data requires the complete cloud mask, ice mask, and 11 μm BT (0.64 μm reflectance) image, the AIM need be implemented towards the end of the processing chain, after the entire image is processed. The AIM also needs the image from 24 hours prior.

5.3 Quality Assessment and Diagnostics

The following procedures are recommended for diagnosing the performance of this algorithm.

- Check input data including BTs, reflectance, cloud mask, and land mask.
- Monitor the products with products from other dataset and real time in-situ observations.
- Periodically image the outputs to look for artifacts or non-physical behaviors.
- Maintain a close collaboration with users, which use the output of this algorithm in their product generation and other applications.

5.4 Exception Handling

This algorithm includes checking the validity of input data before running and setting quality flag for the input data and output product. This algorithm also checks for missing input variables values. This algorithm currently does not have any graceful degradation. If the input channels, cloud mask or ice mask is missing, then the algorithm will not run.

5.5 Algorithm Validation

The current validation cases are based on comparisons with ice motion products from buoy observations. Such validations will continue using MODIS, model wind fields,

drifting ice buoys, and other proxy data sets over the Arctic Ocean. Validations with products from other satellites, e.g. AVHRR, SAR, passive microwave, will help. Further validation over mid-latitude will be carried out when in situ observations become available.

6 Assumptions and Limitations

The following sections describe the current limitations and assumptions in the current version of the AIM.

6.1 Assumptions

The following assumptions have been made in developing and estimating the performance of the AIM.

1. The cloud mask provides an accurate clear sky mask for both the current and scene 24 hours prior are available in a timely manner.
2. Land mask maps are available to identify land/water pixels and is available at pixel level
3. Sensor data for the 11 μm band (0.64 μm band) is available for the current and scene 24-hour prior in a timely manner.
4. All data is in the same gridded format and in the same orientation.

All the inputs are required to run this algorithm. If land mask is not available, any global land mask at the GOES-R ABI pixel resolution can be used.

6.2 Assumed Sensor Performance

We assume the sensor will meet its current specifications. However, the AIM will be dependent on the following instrumental characteristics.

- The cross correlation of each search bin in AIM will be critically dependent on the amount of striping in the data.
- Unknown spectral shifts in some channels will cause biases in calculation of the cross-correlations and may impact the performance of the AIM.
- The AIM is critically dependent on the quality of the cloud mask, ice mask, as well as 11 μm sensor data.
- Errors in navigation from image to image will affect the re-mapping of the data into pixel space.
- All sensor issues can play a role in accurate clear sky detection. In addition, it is assumed that the cloud mask is an accurate portrayal of clear/cloudy pixels.

6.3 Planned Product Improvements

To improve this algorithm various modifications are being investigated:

- Size of the sub-window will be tested to get the best results. Current size of the search window is 15 pixel by pixel.
- The maximum allowable displacement in pixel space can still be optimized.
- Rewrite the core ice motion routine to operate in latitude/longitude coordinates rather than image coordinates and eliminate the post-processing routine that was added in 2018.

7 References

Emery, W.J., C.W. Fowler, J. Hawkins, and R.H. Preller, 1991. Fram Strait satellite image derived ice motions, *J. Geophys. Res.*, 96, 4751-4768.

Fowler, C. 2003, updated 2007. *Polar Pathfinder Daily 25 km EASE-Grid Sea Ice Motion Vectors*. Boulder, Colorado USA: National Snow and Ice Data Center. Digital media.

Maslanik, J., C. Fowler, J. Key, T. Scambos, T. Hutchinson, and W. Emery. 1998. AVHRR-based Polar Pathfinder products for modeling applications. *Annals of Glaciology* 25:388-392.

Schmit, Timothy J., Mathew M. Gunshor, W. Paul Menzel, James J. Gurka, Jun Li, A. Scott Bachmeier, 2005: Introducing the next-generation Advanced Baseline Imager on GOES-R. Bull. Amer. Meteor. Soc., 86, 1079-1096

Thorndike, A. S., and R. Colony (1982), Sea Ice Motion in Response to Geostrophic Winds, J. Geophys. Res., 87(C8), 5845\u20135852, doi:10.1029/JC087iC08p05845.